JOURNAL OF AIRCRAFT
Vol. 47, No. 1, January–February 2010

Engineering Notes

Drag Force Balance of a Blunt and Divergent Trailing-Edge Airfoil

M. El-Gammal*
University of Western Ontario, London, Ontario N6A 5B9, Canada
J. W. Naughton†
University of Wyoming, Laramie, Wyoming 82071
and
H. Hangan‡
University of Western Ontario, London, Ontario N6A 5B9, Canada

DOI: 10.2514/1.46308

Nomenclature

C_d	=	airfoil drag coefficient
C_f	=	skin-friction coefficient
C_l	=	airfoil lift coefficient
C_p	=	pressure coefficient
c	=	airfoil chord length
d	=	trailing-edge thickness
Re	=	Reynolds number
U_o	=	freestream velocity
x, y, z	=	coordinate directions
α	=	angle of attack
ϑ	=	local surface slope angle

I. Introduction

Modifying the trailing edge of an airfoil can lead to significant improvements in its aerodynamic performance. Divergent trailing-edge (DTE) airfoils were first introduced to improve the lift-to-drag ratio of supercritical airfoils at cruise conditions for commercial aircraft [1]. They are a natural evolution of Gurney flaps used on low-speed airfoils to increase airfoil lift and reduce profile drag [2]. DTE airfoils are characterized by upper and lower surfaces that diverge from each other over about the aft 30% of chord forming a blunt trailing. This DTE approach was extended to low-speed applications such as wind turbine blades [3]. DTE profiles on wind turbine blades can improve aerodynamic performance and structural strength compared to profiles with sharp trailing edges. Critical to enhancing the aerodynamic performance of these airfoils and optimizing their geometrical configuration is the accurate characterization of surface flow properties as well as the precise determination of their aerodynamic characteristics.

Received 13 July 2009; accepted for publication 2 November 2009.

*Graduate Research Assistant, Boundary Layer Wind Tunnel Laboratory; currently Postdoctoral Fellow, Department of Mechanical Engineering, McMaster University, Hamilton, Ontario L8S4L8, Canada.

†Associate Professor, Department of Mechanical Engineering, University of Wyoming, 1000 East University Avenue. Associate Fellow AIAA.

‡Professor and Director, Boundary Layer Wind Tunnel Laboratory.

The profile drag of airfoils can be determined using three different approaches: dynamic force balance, wake surveys, and direct measurements of the two drag components, that is, skin friction and pressure drag. Direct measurements of drag components along the airfoil surface also provide useful information for characterizing the surface flow (i.e., the boundary-layer state). However, the accuracy of the available direct skin-friction measurement methods was previously questioned [4]. Recently, the oil film interferometry method that relies on local thinning of an oil film under shear stress has been proven to accurately measure skin friction [5].

In the present study, direct measurements of both surface pressure and skin friction are employed to 1) characterize the physics of the surface flow around a DTE airfoil, and 2) estimate accurately the profile drag from direct measurements and compare it with that estimated from a survey in the airfoil far wake.

II. Experimental Setup

The DTE airfoil used in the present experiments (see Fig. 1) is described by Thompson and Lotz [6]. The airfoil surface coordinates were chosen to match the distribution of surface pressure, momentum thickness, and shape factor over the aft 20% of the chord to those on the DTE Douglas Long Beach Airfoil DLBA 243 in transonic flight. The model is constructed from a conventional glass-fiber reinforced composite sandwich based on the method described by Rutan [7]. Both airfoil surfaces were tripped at 5% downstream of the leading edge by installing surface protrusions of 2 mm in diameter, 1 mm in height, and spaced 5 mm apart in the cross-stream direction.

The experiments were conducted in the open-return circuit wind tunnel BLWTL I at the Boundary Layer Wind Tunnel Laboratory, located at the University of Western Ontario. The dimensions of the rectangular test section are 1.7 m in height, 2.4 m in width, and 33 m in length, allowing for measurements in the airfoil's far wake region. The airfoil model was mounted upstream of the testing section, at a distance of 5 m downstream of tunnel inlet using two straight and rigid flat supporting plates of 2.6 m in length and 1.5 m in height. Velocity measurements upstream and in the far wake of the airfoil were obtained with pitot tubes. The experiments were conducted at a U_o of 12.8 m/s $\pm 1\%$, $Re = 1.23 \times 10^6$ based on the airfoil chord length, and $\alpha = 0$ deg. The resultant airfoil lift coefficient estimated from integrating the normal components of the pressure and skin-friction coefficients along the airfoil surface was $C_l = 0.486$.

The mean pressure distribution around the airfoil was obtained by using three separate spanwise rows of 79 pressure taps each, located at $z/c = 0$ and ± 0.017. The pressure taps' diameter was 0.8 mm and they were flush mounted to the surface. They were connected to multichannel Pressure Systems, Inc. model ESP-16 pressure scanners via a PVC tubing system. The frequency response of the tubing system was flat up to 160 Hz. The pressure transducer operating range varied from 0 to 1000 Pa. The pressure measurements were simultaneously sampled at 800 Hz for 300 s and low-pass filtered at a cutoff frequency of 160 Hz. The pressure signal was averaged over 240,000 samples. The pressure system calibration relative errors were less than 1%. The statistical uncertainties for pressure coefficients C_p were not more than 0.3% based on a 95% confidence interval. The pressure measurements gathered from the three pressure tap rows were essentially identical, indicating a quasi-two-dimensional flow behavior [8] (see Fig. 2a).

The oil film interferometry method is based on the concept that, when an oil film on a surface is subjected to shear stress, its thickness will change with time. Thus, if the oil height is measured at one or more times, the skin-friction coefficient C_f can be determined. For each test, oil was applied first on the Mylar film surface as a thin

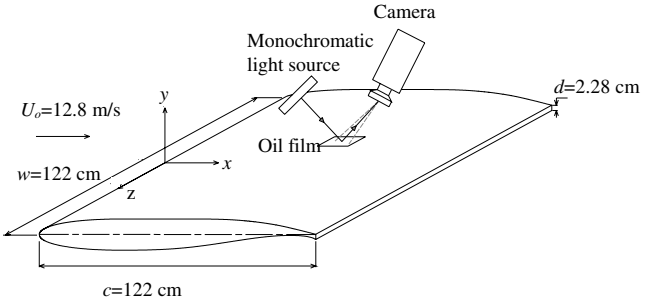

Fig. 1 Schematic diagram of the airfoil geometry and oil film interferometry setup.

continuous line. The oil viscosity used in the tests varied from 20 cS in low surface shear stresses to 100 cS, at which high shear stresses were expected and strong surface curvature existed. After applying the oil film, the wind tunnel was closed and turned on for approximately 10 min. The tunnel was then stopped, and the camera and light were traversed inside the tunnel (see Fig. 1) to obtain an interferogram image. The tunnel temperature was recorded during the tests to correct the oil viscosity for temperature variations. Naughton et al. [5] provide a complete description for determining C_f from the interferograms. The precision uncertainty for each skin-friction value was calculated based on averaging C_f across the model in the z direction and over infinitesimal regions in the x direction. A typical number of averages assigned to any location was 25. Bias uncertainties developed from oil viscosity were significantly reduced by precalibrating the oil viscosity variations versus the temperature. The statistical uncertainty at most of the locations was approximately 4% and did not exceed 7%.

III. Results and Discussion

The measured averaged surface skin-friction and surface pressure coefficients are illustrated in Fig. 2. The present pressure measurements along the airfoil surface are generally in good agreement with those obtained by Thompson and Lotz [6]. The skin-friction results show that the flow is attached everywhere on the airfoil surface.

As the flow accelerates around the airfoil nose, a highly favorable pressure gradient is created, and a laminar boundary layer develops. The skin friction significantly increases and reaches its peak value at $x/c \sim 0.01$ and 0.02, for the suction and pressure sides, respectively, then steeply decreases as the favorable pressure gradient decreases or becomes adverse.

On the airfoil suction side, downstream of the boundary-layer trip (i.e., $x/c = 0.05$), the boundary layer exhibits transition to turbulence and, as a result, a significant increase in the skin friction takes place near $x/c = 0.09$. At locations farther downstream on the suction side, an adverse pressure gradient is exhibited from $x/c =$ 0.05 to 0.4. The adverse pressure gradient reduces the skin-friction coefficient due to the reduction in the streamwise velocity gradient. From $x/c \approx 0.48$ to 0.64, a favorable pressure gradient develops, indicating acceleration in the flow and thus an increase in the skin-friction coefficient. Therefore, a second skin-friction peak is observed at $x/c = 0.68$. Because of the airfoil shape from $x/c \approx$ 0.62 to the trailing edge, the streamlines in the inviscid flow diverge, and an adverse pressure gradient develops again. As a result, the skin friction decreases in this region.

On the airfoil pressure side surface, transition does not occur right after the trip as on the suction side. The existence of the boundary-layer trip on the airfoil pressure side might induce local flow separation reattachment; however, due to the favorable pressure gradient in this case, the overall transition is delayed compared to the airfoil suction side. On the suction side, the boundary-layer trip along with the adverse pressure gradient combine to promote earlier boundary-layer transition [9]. Downstream, on the pressure side, the flow streamlines in the inviscid flow diverge due to the airfoil shape. As a result, an adverse pressure gradient develops, that is, $x/c=$ 0.42–0.97; thus, the skin-friction values drop. Further downstream,

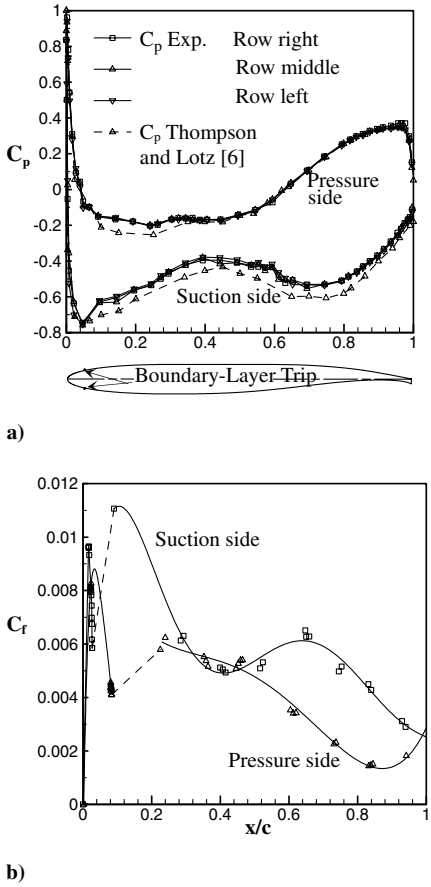

Fig. 2 Averaged surface properties: a) pressure coefficient, and b) skin-friction coefficient.

due to the favorable pressure gradient developed by the divergent trailing-edge configuration, the skin friction increases.

It is observed from the measurements, except near transition, that the skin friction and pressure are inversely related and that the skin friction responds to even slight changes in the pressure gradient. Such information is crucial for design in which the optimization of lift and drag simultaneously requires such information.

The profile drag has been calculated from both direct measurements and wake surveys. The profile drag coefficient C_d calculated from the surface measurements along both the suction and pressure airfoil surfaces is estimated using

$$C_d = \int_0^1 C_p \tan\vartheta \, \mathrm{d}\frac{x}{c} + \int_0^1 C_f d\frac{x}{c}$$

Wake survey measurements have been conducted in the airfoil far wake at $x/c = 3.8c$ downstream of the airfoil trailing edge, where the wake flow reaches a self-similar state [8], is quasi two dimensional [10], and the wake static pressure is approximately similar to the freestream static pressure [8]. The profile drag and, thus, C_d were determined from wake measurements based on the method described in [11].

Table 1 illustrates the airfoil drag coefficient calculated from both direct measurements and wake survey along with uncertainty values. The uncertainty of the skin-friction drag is developed from various possible polynomial data fitting. The results indicate that the skin-friction drag and pressure drag comprise approximately 40 and 60% of the airfoil total drag, respectively, indicating that both drag components have a comparable contribution to the airfoil total drag at the test conditions investigated. The average airfoil base drag comprises 10% of the airfoil total drag. Furthermore, along the airfoil suction side, the pressure on the airfoil nose balances pressure recovery to some extent, thus resulting in a negative drag contribution. When

Table 1 Drag coefficients from direct measurements of pressure and skin friction and from a far wake survey

	Airfoil drag	Airfoil region	C_d	C_d total
Direct measurements	Skin-friction drag	Suction side	$0.0059 \pm 4.2\%$	$0.0099 \pm 3.85\%$
		Pressure side	$0.004 \pm 3.35\%$	
	Pressure drag	Suction side	$-0.00153 \pm 1\%$	$0.0147 \pm 1\%$
		Pressure side	$0.0137 \pm 1\%$	
		Base	$0.0025 \pm 1\%$	
	Total C_d		$0.0246 \pm 2\%$	
C_d, wake survey at 3.8c			$0.023 \pm 1\%$	
Variation %			6.5%	

the components are summed, the direct measurements of drag and that determined from the wake survey match within 6.5%.

IV. Conclusions

The surface flow and the profile drag of an airfoil with a blunt and divergent trailing edge was experimentally investigated. Accurate skin-friction and pressure coefficient distributions over the entire chord of the airfoil were obtained using oil film interferometry and surface pressure measurements, respectively. The skin-friction measurements along the airfoil suction side clearly showed the boundary-layer transition just downstream of the boundary-layer trip, but this scenario did not take place at the corresponding location of the airfoil pressure side. The total profile drag coefficient determined by a direct integration of surface skin and pressure coefficients agreed quite well with the drag determined using a momentum integral approach with a velocity profile from the airfoil far wake.

References

[1] Henne, P. A., "Innovation with Computational Aerodynamics: The Divergent Trailing-Edge Airfoil," *Applied Computational Aerodynamics*, AIAA, Washington, DC, 1990, pp. 221–261.

[2] Liebeck, R. H., "Design of Subsonic Airfoils for High Lift," *Journal of Aircraft*, Vol. 15, 1978, pp. 547–561. doi:10.2514/3.58406

[3] Standish, K. J., van Dam, C. P., "Aerodynamic Analysis of Blunt Trailing Edge Airfoils," *Journal of Solar Energy Engineering*, Vol. 125, 2003, pp. 479–487. doi:10.1115/1.1629103

[4] Naughton, J. W., and Sheplak, M., "Modern Developments in Shear-Stress Measurement," *Progress in Aerospace Sciences*, Vol. 38, 2002, pp. 515–570. doi:10.1016/S0376-0421(02)00031-3

[5] Naughton, J. W., Viken, S. and Greenblatt, D., "Skin-Friction Measurements on the NASA Hump Model," *AIAA Journal*, Vol. 44, 2006, pp. 1255–1265. doi:10.2514/1.14192

[6] Thompson, B. E., and Lotz, R. D., "Flow Around a Blunt and Divergent Trailing Edge," *Experiments in Fluids*, Vol. 33, 2002, pp. 374–383.

[7] Rutan, B., *Moldless Composite Homebuilt Sandwich Aircraft Construction*," 3rd ed., Rutan Aircraft, Mojave, CA, 1983.

[8] El-Gammal, M., and Hangan, H., "Three-Dimensional Wake Dynamics of a Blunt and Divergent Trailing Edge Airfoil," *Experiments in Fluids*, Vol. 44, 2008, pp. 705–717. doi:10.1007/s00348-007-0428-6

[9] Tani, I., "Boundary-Layer Transition," *Annual Review of Fluid Mechanics*, Vol. 1, 1969, pp. 169–196. doi:10.1146/annurev.fl.01.010169.001125

[10] Bell, J. H., Mehta, R. D., "Measurement of Streamwise Vortical Structures in a Plane Mixing Layer," *Journal of Fluid Mechanics*, Vol. 239, 1992, pp. 213–248. doi:10.1017/S0022112092004385

[11] White, F. M., *Fluid Mechanics*, 4th ed., McGraw–Hill, New York, 1998, Chaps. 3, 7.